

## ARTICLES

## Study of Cobalt-Filled Carbon Nanoflasks

Suwen Liu,<sup>†,||</sup> Seth Boeshore,<sup>‡</sup> A. Fernandez,<sup>§</sup> M. J. Sayagués,<sup>§</sup> J. E. Fischer,<sup>‡</sup> and Aharon Gedanken<sup>\*,†</sup>

Department of Chemistry, Bar-Ilan University, Ramat-Gan 52900, Israel, Laboratory for Research on the Structure of Matter, University of Pennsylvania, Instituto de Ciéncia de Materiales de Sevilla and Departamento Química Inorganica, Centro de Investigaciones Científicas Isla de la Cartuja, Spain, and Department of Applied Chemistry, University of Science and Technology of China, Hefei, Anhui 230026, People's Republic of China

Received: January 7, 2001; In Final Form: May 16, 2001

A new form of fullerene-type carbon, named carbon nanoflasks, is described in this paper, using  $\text{Co}(\text{CO})_3\text{NO}$ , a special precursor, in their synthesis. Upon its decomposition, the  $\text{Co}(\text{CO})_3\text{NO}$  is not only a source of carbon, but also gives rise to fcc cobalt particles, whose size can grow from several nanometers to hundreds of nm in the course of the decomposition. After a careful purification process, the percentage of cobalt-filled carbon flasks can be as high as 30%. The width of the flask tube-necks ranges from 50 nm to over 100 nm, while the body of the flask ranges from 100 nm to 500 nm, and in some cases reaches over 1  $\mu\text{m}$ . HRTEM reveals that the graphitic layers of the flask walls are usually over 100 nm thick, and are much thicker than the flask cap. After an acid treatment of the sample, opened and empty carbon flasks can be easily obtained. XRD, TEM, SEM, XPS, AFM, and SQUID measurements were employed in the characterization of the flasks. An explanation of the formation of the carbon nanoflasks is proposed in this paper.

## Introduction

Phenomenal progress has been made in the science of carbon nanotubes (CNT) since the publication of Iijima's landmark paper in 1991.<sup>1</sup> A variety of novel structures with trigonally bonded carbons have been discovered: single-walled nanotubes<sup>2</sup> (SWCNT), nested spheroidal shell (onions),<sup>3</sup> giant fullerene shells,<sup>4</sup> interconnected fullerene-like cages,<sup>5</sup> cross-linked graphitic cages,<sup>6</sup> flattened nanotubes, and flattened carbon nanoshells.<sup>7,8</sup> Strong interest in these materials has been aroused in the field of nanotechnology<sup>9</sup> when it became possible to insert different kinds of materials with potentially interesting properties into the core volume of the CNT or carbon nanoparticles.

Different methods of synthesis have been attempted and various encapsulated materials have been tested,<sup>10</sup> in particular those involving magnetic or ferromagnetic materials.

Cobalt-filled carbon nanoparticles or nanotubes were recently prepared and studied by several groups.<sup>11–19</sup> Guerret-Plecourt and co-workers reported the preparation of cobalt nanowires encapsulated in nanotubes.<sup>11</sup> They used the arc-discharge method for their fabrication. The same group later demonstrated that a sulfur impurity (of approximately 0.25%), caused the filling of nanotubes with various materials.<sup>19</sup> Their cobalt nanowires,

however, were short, having only a 200 nm length. Organo-metallic precursors were successfully used as sources for the carbon and the metal, and yielded carbon nanotubes; some of them filled with materials.<sup>20–22</sup>

In a previous paper we reported the existence of multishelled, flask-shaped carbon nanostructures whose overall geometry differs from that of carbon nanotubes or carbon nanoparticles. We called these carbon vessels "carbon nanoflasks".<sup>24</sup> The carbon nanoflasks were described as a new form of fullerene-type carbon that gave a fascinating image.<sup>25</sup> To better understand the properties of the carbon nanoflasks, they have been purified carefully and repeatedly. In the purified products, the percentage of the cobalt-filled nanoflasks of all the observed TEM structures is now over 30%, which is much higher than the 10–15% in the original paper. Some new results on these cobalt-filled carbon nanoflasks (CoCNF) are reported in the current paper.

## Experimental Section

The synthesis is carried out in a 2 mL closed vessel cell, which is assembled from a stainless steel Swagelok parts. A  $3/8$  in. union part was capped from one side by a standard plug. For this synthesis, 400 mg of magnesium powder and 700 mg of  $\text{Co}(\text{CO})_3\text{NO}$  were placed in a cell at room temperature. The vessel is then immediately closed tightly because  $\text{Co}(\text{CO})_3\text{NO}$  is an air-sensitive material, and is heated at 900 °C for 3 h. The reaction takes place at the autogenic pressure of the precursors. After cooling to room temperature, we do not detect a release of pressure from the vessel. The products are treated with 50 mL of 8 M HCl at 70 °C for 1 h, and then left overnight in the

\* Corresponding author. E-mail: gedanken@mail.biu.ac.il. Phone: 0972-3-5318315. FAX: 0972-3-5351250.

<sup>†</sup> Department of Chemistry.

<sup>‡</sup> Laboratory for Research on the Structure of Matter.

<sup>§</sup> Instituto de Ciéncia de Materiales de Sevilla and Departamento Química Inorganica.

<sup>||</sup> Department of Applied Chemistry.

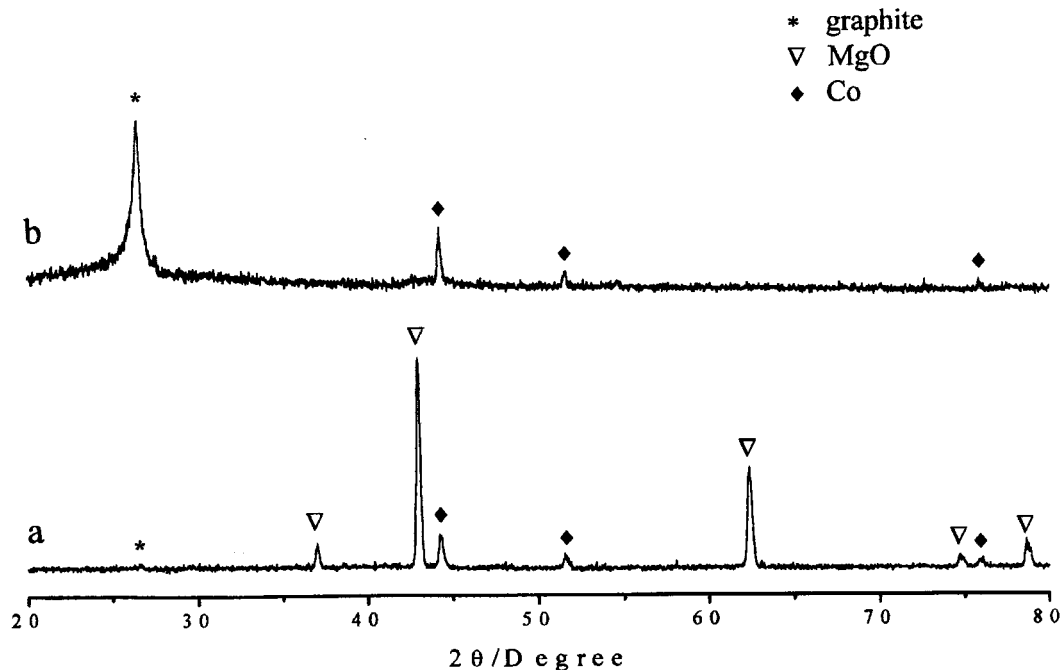


**Figure 1.** X-ray diffraction pattern of the sample: (a) as-prepared sample; (b) after treatment with concentrated HCl.

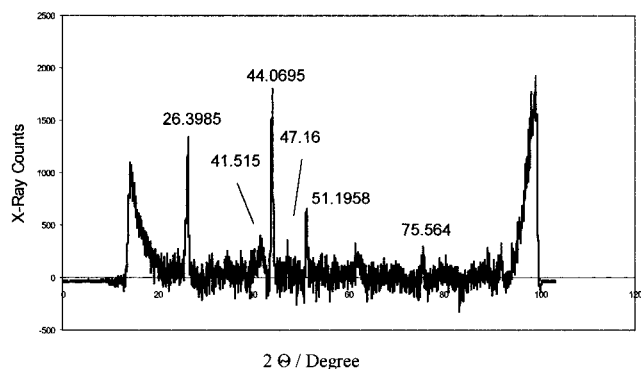


**Figure 2.** XRD data for a sample after purification and in the air-opened condition for three months. The peaks at  $44.0695^\circ$ ,  $51.1958^\circ$ , and  $75.564^\circ$  are due to fcc cobalt. The peaks at  $41.515^\circ$  and  $47.16^\circ$  are caused by hcp cobalt. The peak at  $26.3985^\circ$  is graphite.

acid at room temperature. Finally, a black, soot-like product is obtained after filtering and washing processes.

This product contained unfilled nanotubes, amorphous carbon, and cobalt-filled carbon nanoparticles.<sup>23</sup> To purify this blend, the material is placed in a vial filled with ethanol and is sonicated for 30 min. This procedure is necessary to untangle the unpurified material. The sonicated sample is placed in a strong magnetic field using an  $\text{SmCo}_5$  magnet. This is done because the unpurified material responded to a magnetic field; it is assumed that amorphous carbon and unfilled nanotubes, if untangled, would not be attracted to a magnet. In the presence of the field, the magnetic Co-filled materials aggregate along field lines. These materials are removed from the vial and placed in a second vial filled with ethanol. The procedure of sonication followed by magnetic separation is repeated on the second vial. This process yielded the purified materials that were subjected to X-ray diffraction (XRD), high-resolution electron microscopy (HREM), scanning electron microscopy (SEM), atomic force microscopy (AFM), X-ray photoelectron spectroscopy (XPS), magnetic force microscopy (MFM), and superconducting quantum interference device (SQUID).

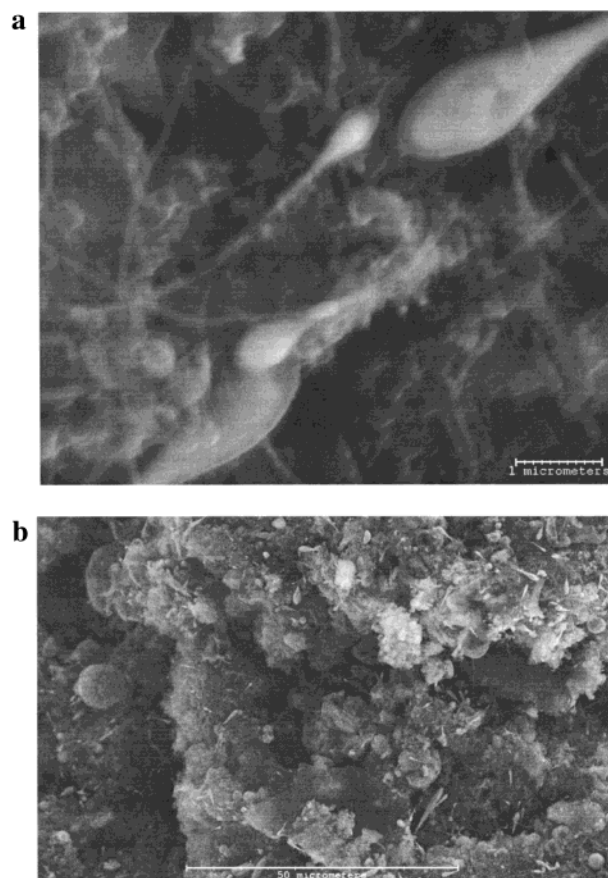


**Figure 3.** (a) SEM image of a single CoCNF resting on top of an assortment of other CoCNF and unfilled nanotubes. Note that the cobalt core (lighter gray) is visible within the carbon shell. (b) SEM image of bulk material at 800x magnification. The CoCNF can be seen resting on top of the amorphous carbon.

## Results and Discussion

**1. X-ray Diffraction and Chemical Reactions.** The as-prepared powder is characterized by X-ray powder diffraction

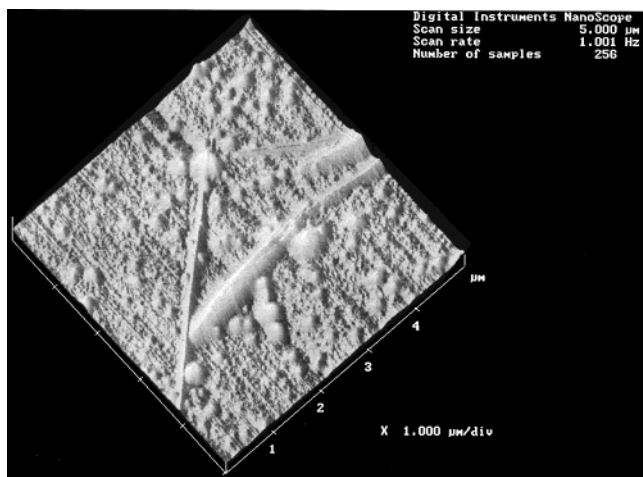
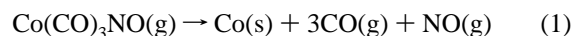


**Figure 4.** MFM image of four carbon nanoflasks.

(Figure 1a), and the main peaks are identified as those of MgO (JCPDS 45-946) and fcc metallic cobalt (JCPDS 15-806). After dissolving the powder in concentrated HCl (8 M), MgO and most of metallic cobalt features disappeared. Thereby, the graphite peak became the dominant peak (Figure 1b), while the fcc cobalt patterns reveal weaker diffraction peaks (hcp cobalt was not found). However, after carefully purifying the products

as described above, fcc cobalt patterns became the dominant peaks (See Figure 2), which are much higher than those in Figure 1b. This reveals that a large percentage of cobalt is encapsulated in the carbon nanoflasks after the careful purification process. The result, shown in Figure 2, was measured after the sample was left in the open air for three months at room temperature. Only very weak hcp cobalt diffraction peaks are detected. We consider the walls of the nanoflasks and nanotubes as hindering the conversion of the fcc Co to the stable hexagonal phase. It further proved that fcc structured cobalt, which exists only in high temperature (above 450 °C), can exist and be stable inside the carbon nanoflasks stably.

On the basis of the XRD patterns, the following mechanism is proposed. In the first step,  $\text{Co}(\text{CO})_3\text{NO}$  is decomposed into Co, CO, and NO. Subsequently, CO reacts with Mg to yield MgO and carbon. The reactions are as follows:



During carbon formation, Co plays the role of a catalyst for the creation of nanotubes. At the same time, part of the metallic Co produced by the decomposition of the precursor is encapsulated in the carbon shells. Briefly, these  $\text{Co}(\text{CO})_3\text{NO}$  molecules, on decomposition, act not only as a source of carbon,

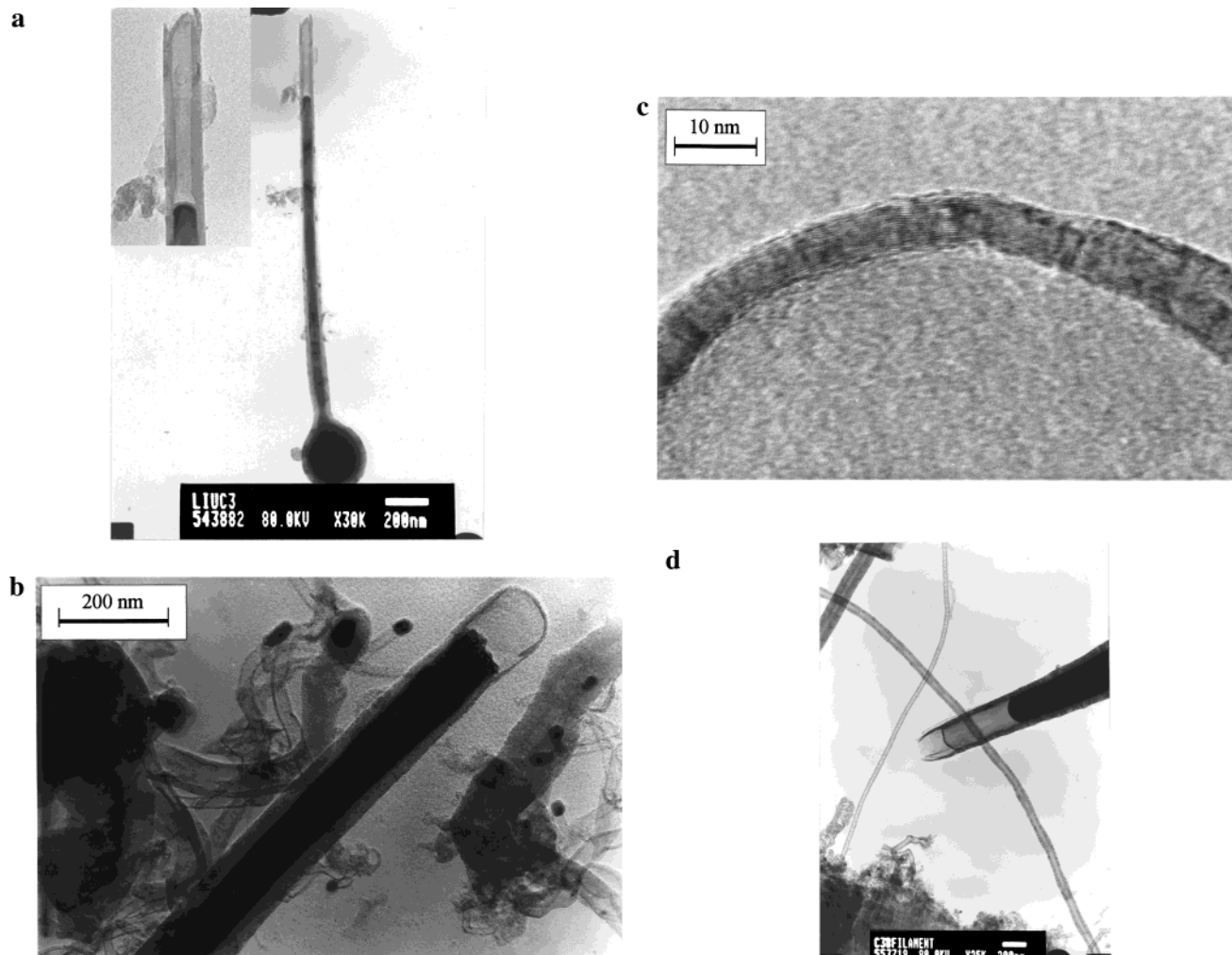


**Figure 5.** (a) An individual carbon nanoflasks filled with Co. The inset is a close-up of the top part of this flask. Scale bar 200 nm. (b) Another individual carbon nanoflasks filled with Co, there is only one cap in the top. (c) A HRTEM image of the cap. It shows that there are about 20 layers of graphite in the cap. (d) One flask with only an inner cap.

but also give rise to small metal clusters or particles which function act as catalysts for the formation of the carbon nanotubes or nanoflasks.

**2. SEM, AFM, and XPS.** JEOL 6300F and 6400 scanning electron microscopes were used for the observation of bulk samples and individual carbon nanoflask. SEM images reveal that the sizes and shapes of the carbon materials are quite different from the usual carbon nanotubes. In fact, the only feature that all the carbon materials have in common is an enlarged head, making the tubes appear similar to baby tadpoles (Figure 3a). It is clear in this picture that the cobalt core (lighter gray) is visible within the carbon shell. XRD results reveal that these nanovessels were filled with fcc cobalt. The nanoflasks have an ovoid or a spherical bulbous base with a "plus end" from which the nanotube grows, lengthening one-dimensionally. In some cases, the cobalt was only in the bottom of the flask and the tube-neck is hollow. In others, the cobalt core filled the entire length of the nanoflask. Figure 3b shows a large amount of flask-shaped carbon in the products. The percentage of flask-shaped materials is much higher than that in our previous report.<sup>24</sup> We roughly estimate that the flask-shaped materials are over 30% of the product. Obviously, the increase should be attributed to the better purifications methods described in the Experimental Section. X-ray spectroscopy at 15 keV centered on an individual flask yielded the atomic percentages of 83.45 and 16.57 for carbon and cobalt, respectively.

The width of the tube-necks of the flasks ranged from 50 nm to over 100 nm. The body of the flask is often more than twice the width of the tube, but in some cases it reached over 1  $\mu\text{m}$  in size. It is common for the cobalt core to end and then resume farther down along the tube, as seen in Figure 3a. Usually, when a cobalt core is present the tube is very straight. When the core ends, the remaining length sometimes becomes curved.

Atomic force microscopy (AFM) was used to topographically map the cobalt-filled nanoflasks. Magnetic force microscopy (MFM) is also used in an attempt to find the magnetic response to the domain structure of the cobalt core. This procedure is similar to AFM, except that a magnetic tip is used to probe the sample. However, the MFM measurements are not so helpful for such CoCNFs (cobalt carbon nanoflasks). The response of the products to the magnetic tip is not very apparent. Only after much data manipulation was it possible to see the response. Figure 4 is a topographical image obtained from MFM measurements. The resolution of the image is decreased compared to the AFM image because of a thicker magnetic tip was used.

X-ray photoelectron spectroscopy (XPS) was employed with an AXIS, HIS, 160, ULTRA apparatus. The XPS spectrum detected only pure carbon (no Co signal). This result seems not consistent with both the SEM and XRD results. The obvious reason for the absence of the cobalt spectrum is due to the fact the XPS monitors mostly the surface area. The outer cobalt layer can be found as deep as several nanometers from the surface, and therefore, it is not observed in the XPS spectrum.

**3. A Close-up of Carbon Nanoflasks and Removing Their Caps.** Figure 5a shows an individual carbon nanoflask, which is almost fully filled with Co. Only a small part near the top is empty. The inset depicts a close-up of the top of this flask. It is found that two caps cover this nanoflask. One is an inner cap, which is on the end of nanowires and covers the tip tightly. Only some of the nanoflasks have inner caps. The second is an outer cap that covers the tube end at the top of the flask. Figure 5b shows an imaging of the top part of a flask. Obviously, there

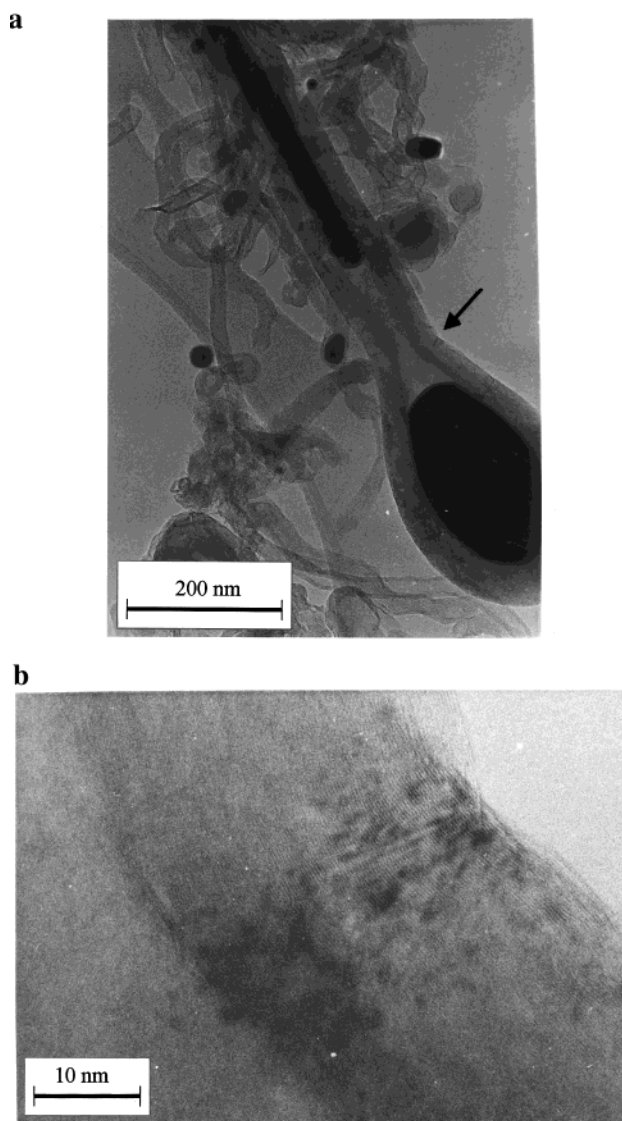


**Figure 6.** (a) An open and empty nanoflask was formed after a treatment of 8 M HCl. A cobalt-filled carbon nanoflask. The part shown by an arrow was empty. (b) Scale HREM image of the arrow marked site in Figure 6a.

is only an outer cap covering the flask. The HREM image revealed that the cap was composed of about 20 layers of graphite (Figure 5c). In addition, we also found a small amount of flasks with only inner caps. Figure 5d shows such a cap. Usually, the thickness of the cap is much thinner than the walls of the flask body. This result implied that the cap could be easier to break or remove than the wall of the flasks. Follow-up experiments and results confirmed that our above prediction was correct.

We previously reported that when the as-prepared sample was further treated with an aqueous solution of  $\text{H}_2\text{SO}_4$  and  $\text{H}_2\text{O}_2$  under ultrasonic irradiation for 2 h, some of flask caps were removed.<sup>24</sup> The bodies of the nanoflasks, however, were unaffected. This process also caused the dissolution of the cobalt and the flasks became empty. This result revealed that the nanoflasks sustaining the sonication, remained intact and are firm nanovessels. In fact, we have also found a very small amount of empty nanoflasks in the as-prepared products (treated only by 8 M HCl as description in the Experimental Section). Figure 6a shows two empty flasks in the as-prepared sample, one was opened at the cap; surprisingly, the other was opened

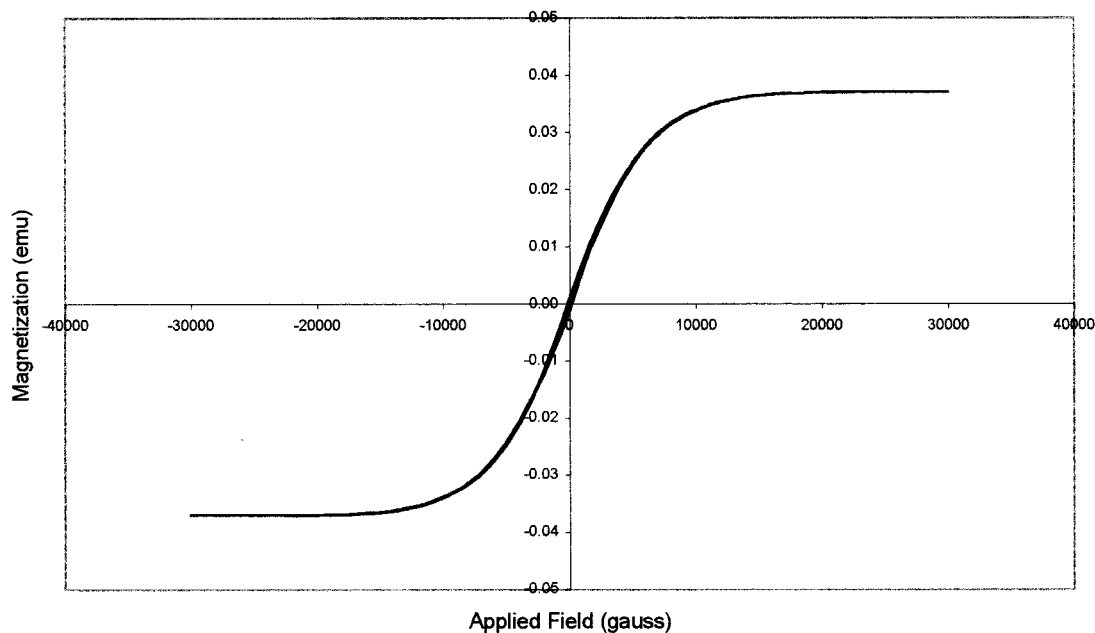


**Figure 7.** Hysteresis loop for the magnetization of cobalt, taken at 50 K. Best-fit line created using data points. Note the magnetization at zero field; it is almost zero.

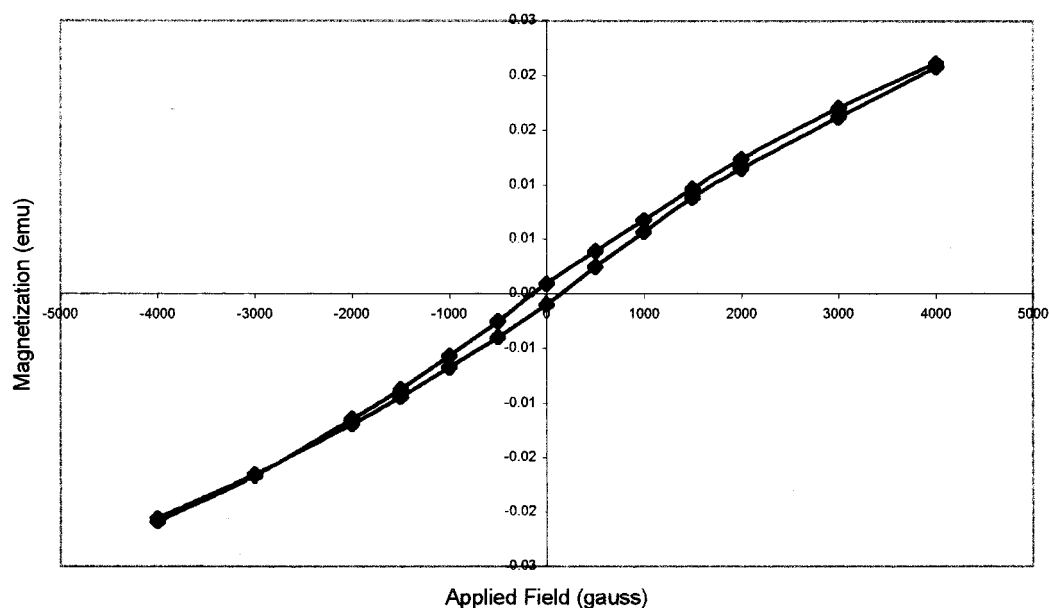


**Figure 8.** Hysteresis loop for the magnetization of cobalt, taken at 50 K. It has been expanded to show the low-field response of the CoCNF.

in the neck. Most of empty flasks were opened at the cap. One of the reasons is the cap is much thinner than the flask wall. Another reason is that the strain at the cap and the presence of pentagons help to initiate an oxidation process. The degree of curvature, e.g., the strain, between the caps and body of the nanoflasks is different. So, although pentagons might play a role, strain must be the key factor in the onset of oxidation at the top of the nanoflasks.

Figure 6a shows an interesting individual carbon nanoflask, with filled cobalt in the both of bottom and tube-neck of the flask, while there is no Co in the connection part between the bottom and the tube-neck. The wall shown by an arrow is observed by HREM. Figure 6b is the HREM image of the connection between the flask body and the tube-neck. There are about 100 layers of graphite in the area. As can be seen in Figure 6a, the wall thickness in the lowest bottom of this flask is much thicker than that in other places. It should be pointed

out that empty nanoflasks have never been found in any of the crude products (before HCl treatment). The implication of this result is that the as-prepared carbon nanoflasks are always filled with cobalt.

**4. Superconducting Quantum Interference Device Measurements.** One of the main goals of this research is learning more about the cobalt core. It has been theorized that cobalt in its fcc phase becomes nonmagnetic.<sup>26</sup> Because MFM was unable to yield viable data for the magnetization of cobalt, another method was needed. It is assumed that the MFM tip is not sensitive enough to detect the magnetic force. The magnetic measurements of the cobalt core were conducted using a SQUID magnetometer. The sample cannot be free to move within the SQUID chamber. Because of this, a pellet of Co-filled carbon nanoflasks and paraffin is made by mixing approximately 3 mg of the sample and 5 mg of paraffin. The data are acquired for the paraffin pellet of unaligned, unpurified CoCNT.

Six hysteresis loops were obtained; one was measured for temperatures ranging from 50 to 300 K at 50 K intervals. The results of the SQUID measurements clearly show that the sample is being magnetized (Figure 7). The loops for each temperature were almost identically similar.

After plotting the data for the hysteresis loops, it became evident that the area around zero field should be expanded to find the magnetization at zero field (Figure 8). The magnetization was found to be slightly less than 0.001 emu and practically independent of temperature. The interpretation of this result is that the slight magnetization at zero field is caused by the presence of ferromagnetic hcp cobalt particles. The bulk of the magnetic material, however, is fcc cobalt, which behaves like a paramagnetic material.

**5. Growth Mechanism of the Carbon Nanoflasks.** There is widespread agreement about how a nanotube lengthens, once it has nucleated from a metal particle. It seems to be generally accepted that metallic particles act as catalysts for the graphitization of carbon present in the vapor phase. The carbon then forms a hemispherical graphene cap on the metal particle, and the nanotubes grow from such a graphene cap.<sup>27</sup>

The results presented here show that  $\text{Co}(\text{CO})_3\text{NO}$  is a quite special precursor. These molecules, on decomposition, act not only as a source of carbon but also give rise to fcc cobalt particles whose size can grow from several nanometers to hundreds of nm in the course of the  $\text{Co}(\text{CO})_3\text{NO}$  decomposition. These cobalt particles, serve as nucleation centers for the carbon, which is formed by the reduction of the CO residue by the Mg atoms under the reaction conditions. When this process occurs, the growth proceeds by the addition of carbon as atoms, chains and rings.<sup>16</sup> The formation of the filled nanoflasks happens because the cobalt clusters coagulate very fast at the beginning. However, midway through the process the coagulation slows down and the carbon wraps most of the base. At this moment, only a slight edge of the cobalt cluster that is not wrapped by carbon protrudes from the coated particle, so that when cobalt is further deposited, it causes a wire to grow in one-dimension. The carbon follows the wire, and the tube continues growing onto the base along the cylindrical axis. Furthermore, forming a nanotube-neck and, in fact, also forming a multiwalled carbon nanotube seem to require a suitable diameter of catalytic particles. Only when the diameter of the Co core is smaller than a certain value can the nanotube-necks be formed. Usually, the diameter of cobalt nanowires in the necks is smaller than 100 nm.

## Conclusion

High percentages of CoCNFs were prepared and characterized in this paper. The shapes of the carbon flasks are quite different from the usual carbon nanotubes. After the thinner caps of the

CoCNFs are removed by acid treatment, the empty carbon nanoflasks can be recovered. SQUID measurements clearly show that the fcc cobalt within the tubes is paramagnetic. Also, many of the CoCNFs have cores that end far before the length of the nanotube. This core space is much larger than normal carbon nanotubes and could potentially be used for the storage of materials.

**Acknowledgment.** Dr. Suwen Liu thanks The Fred and Barbara Kort Sino-Israel Postdoctoral Fellowships Foundation for financial support and the China Scholarship Council for their support. Profs. J. E. Fischer and A. Gedanken gratefully acknowledge the receipt of a NEDO International Joint Research Grant. We thank Dr. Shifra Hochberg for editorial assistance.

## References and Notes

- (1) Iijima, S. *Nature* **1991**, *354*, 56.
- (2) Iijima, S.; Ichihashi, T. *Nature* **1993**, *363*, 603.
- (3) Ugarte, D. *Nature* **1992**, *359*, 707.
- (4) Bourgeois, L. N.; Bursill, L. A. *Philos. Mag. A* **1997**, *76*, 753.
- (5) Iijima, S.; Wakabayashi, T.; Achiba, Y. *J. Phys. Chem.* **1996**, *100*, 5839.
- (6) Amaratunga, G. A. J.; Chhowalla, M.; Kiely, C. J.; Alexandrou, I.; Aharonow, R.; Devenish, R. M. *Nature* **1996**, *383*, 321.
- (7) Chopra, N. G.; Benedict, L. X.; Crespi, V. H.; Cohen, M. L.; Louie, S. G.; Zettl, A. *Nature* **1995**, *377*, 135.
- (8) Bourgeois, L. N.; Bursill, L. A. *Chem. Phys. Lett.* **1997**, *277*, 571.
- (9) Ruoff, R. S. *Nature* **1994**, *372*, 731.
- (10) Sloan, J.; Cook, J.; Green, M. L. H.; Hutchison, J. L.; Tenne, R. J. *Mater. Chem.* **1997**, *7*, 1089.
- (11) Guerret-Plecoart, C.; Le Bouar, Y.; Loiseau, A.; Pascard, H. *Nature* **1994**, *372*, 761.
- (12) Seraphin, S.; Zhou, D.; Jiao, J. *J. Appl. Phys.* **1996**, *80*, 2097.
- (13) Lafdi, K.; Chin, A.; Ali, N.; Despres, J. F. *J. Appl. Phys.* **1996**, *79*, 6007.
- (14) Jiao, J.; Seraphin, S.; Wang, X.; Whitters, J. C. *J. Appl. Phys.* **1996**, *80*, 103.
- (15) Kiang, C-H.; Goddard, W. A.; Beyers, R.; Salem, J. R.; Bethune, D. S. *J. Phys. Chem.* **1994**, *98*, 6612.
- (16) Harris, P. J. F.; Tsang, S. C. *Chem. Phys. Lett.* **1998**, *293*, 53.
- (17) Rao, C. N. R.; Govindaraj, A.; Sen, R.; Satishkumar, B. C. *Mater. Res. Innovat.* **1998**, *2*, 128.
- (18) Terrones, M.; Grobert, N.; Zhang, J. P.; Terrones, H.; Olivares, J.; Hsu, W. K.; Hare, J. P.; Cheetham, A. K.; Kroto, H. W.; Walton, D. R. M. *Chem. Phys. Lett.* **1998**, *285*, 299.
- (19) Demoncy, N.; Stephan, O.; Brun, N.; Colliex, C.; Loiseau, A.; Pascard, H. *Eur. Phys. J. B* **1998**, *4*, 147.
- (20) Rao, C. N. R.; Govindaraj, A.; Sen, R.; Satishkumar, B. C. *Mater. Res. Innovations* **1998**, *2*, 128.
- (21) Sen, R.; Govindaraj, A.; Rao, C. N. R. *Chem. Mater.* **1997**, *9*, 2078.
- (22) Sen, R.; Govindaraj, A.; Rao, C. N. R. *Chem. Phys. Lett.* **1997**, *267*, 276.
- (23) Liu, S.; Zhu, J.; Mastai, Y.; Felner, I.; Gedanken, A. *Chem. Mater.* **2000**, *12*, 2205.
- (24) Liu, S.; Tang, X.; Yin, L.; Kolytipin, Y.; Gedanken, A. *J. Mater. Chem.* **2000**, *10*, 1271.
- (25) A private communication with Prof. Eiji Osawa.
- (26) Yoo, C. S.; Cynn, H.; Söderlind, P.; Iota, V. *Phys. Rev. Lett.* **2000**, *84*, 4132.
- (27) Dai, H.; Rinzler, A. G.; Nikolaev, P.; Thess, A.; Colbert, D. T.; Smalley, R. E. *Chem. Phys. Lett.* **1996**, *260*, 471.